Observation of Interband Pairing Interaction in a Two-Band Superconductor: MgB_2

J. Geerk,[1] R. Schneider,[1] G. Linker,[1] A. G. Zaitsev,[1] R. Heid,[1] K.-P. Bohnen,[1] and H. v. Löhneysen[1,2]
[1]*Forschungszentrum Karlsruhe, Institut für Festkörperphysik, P.O.B. 3640, D-76021 Karlsruhe, Germany*
[2]*Physikalisches Institut, Universität Karlsruhe, D-76128 Karlsruhe, Germany*
(Received 20 December 2004; published 9 June 2005)

The recently discovered anisotropic superconductor MgB_2 is the first of its kind showing the intriguing properties of two-band superconductivity. By tunneling experiments using thin film tunnel junctions, electron-coupled phonon spectra were determined showing that superconductivity in MgB_2 is phonon mediated. In a further analysis, which involves first principles calculations, the strongest feature in these spectra could be traced back to the key quantity of two-band superconductivity, the interband pairing interaction. For the phonons, this interaction turns out quite selective. It involves mainly low-energy optical phonon modes, where the boron atoms move perpendicular to the boron planes.

DOI: 10.1103/PhysRevLett.94.227005 PACS numbers: 74.50.+r, 74.25.Kc, 74.70.Ad

The basic mechanism of superconductivity is the formation of Cooper pairs due to the attraction of two electrons via virtual exchange of bosons. In most cases, this coupling is achieved by vibrational excitations (phonons). Electron pairing may in principle occur in two bands of qualitatively different electronic structures crossing the Fermi level, leading to two different energy gaps if impurity scattering between the bands is small enough to preserve clean-limit conditions. A phonon-coupled two-band superconductor is described by three distinct electron-phonon spectral functions, one for each band and one describing the pairing interaction between the bands. Although two-band superconductivity has a long history [1,2], it has only been established clearly in the recently discovered superconducting MgB_2 (transition temperature $T_c = 39$ K) [3]. Here, we report on tunneling spectroscopy on thin films of MgB_2, and determine the tunneling density of states and an effective electron-phonon spectral function accounting for the small energy gap. We identify an unusually strong feature in the tunneling spectrum as the interband pairing interaction and show that superconductivity on the π sheet originates mainly from interband electron-phonon coupling. It is this interband interaction connecting the two foreign Fermi surfaces which is responsible for the exotic properties of the two-band superconductor MgB_2.

Experimental [4] and theoretical studies [5,6] have suggested that superconductivity in MgB_2 is s wave and mediated by electron-phonon coupling. The key quantity in electron-phonon-mediated superconductivity is the Eliashberg function $\alpha^2(\omega)F(\omega)$, where $F(\omega)$ is the phonon density of states and $\alpha^2(\omega)$ is the electron-phonon coupling strength at energy $\hbar\omega$ averaged over directions in k space. For MgB_2 the layered hexagonal lattice structure with boron planes separated by Mg atoms leads to a strongly anisotropic Fermi surface of four separate sheets that are grouped into two-dimensional σ bands and three-dimensional π bands [7,8]. This gives rise to two largely different energy gaps of about 2.5 meV and 7 meV, associated with the π and σ sheets, respectively. Indeed, two gaps of this magnitude have been observed experimentally [9–11]. This grouping implies that the normal and superconducting properties of MgB_2 should be analyzed in terms of an effective two-band model, which essentially contains the three distinct Eliashberg functions $(\alpha^2F)_{\pi\text{-}\pi}$, $(\alpha^2F)_{\sigma\text{-}\sigma}$, and $(\alpha^2F)_{\pi\text{-}\sigma}$ describing the coupling of quasiparticles within the π and the σ band and between the two bands (from now on we will omit the argument ω).

The most direct experimental method for the determination of α^2F is electron tunneling spectroscopy developed by McMillan and Rowell [12]. Briefly, the quantity to be measured via a tunnel junction between the superconductor and a normal metal is the quasiparticle density of states. It contains phonon-induced structures that are observed in the differential conductivity, well above the energy gap region. These structures are used to calculate α^2F via the single-band Eliashberg equations. In the past, this procedure yielded consistent results for many superconductors [13,14]. For a two-band superconductor the data analysis has to be reexamined to include two-band Eliashberg equations [15,16]. In the following, high precision measurements of the phonon-induced structure in the tunneling density of states of MgB_2 are presented along with an analysis based on *ab-initio* local-density approximation (LDA) band-structure results and two-band Eliashberg equations. This gives the proof that MgB_2 is indeed a phonon-mediated superconductor and, even more interestingly, that the dominating feature in the experimental data can be identified as the interband pairing interaction $(\alpha^2F)_{\pi\text{-}\sigma}$.

The junctions of the type MgB_2/insulator/In, Al, or Pb were prepared on thin films of MgB_2 formed by sputtering of boron onto r plane Al_2O_3 substrates which are surrounded by a high-intensity Mg vapor source. Details on thin-film and tunnel-junction preparation are described in Ref. [17]. The films of 200 to 300 nm thickness show transition temperatures between 32 and 34 K as inductively determined. X-ray measurements reveal an expanded c-axis lattice constant of about 0.354 nm due to compressive strain parallel to the substrate surface. The grains of

lateral dimensions of about 100 nm as determined by scanning electron microscopy grow with the c axis perpendicular to the substrate plane with a mosaic spread of about 7 degrees. A natural MgB_2 oxide layer, serving as the barrier in the planar tunnel junctions, was grown at a temperature of 160 °C in ambient air. The junctions with areas between 0.1 and 0.5 mm^2 were completed by evaporation of Pb, In, or Al counterelectrodes and showed resistances between 10 and 150 Ω. The shape of the phonon-induced structures discussed below did not depend on the type of counterelectrode but In was preferred due to its low critical field, which was supplied by an electromagnet. Its remanence field of 5 mT was enough to suppress any Josephson currents for both electrodes in the superconducting state.

In Fig. 1 we display dI/dV versus voltage data of three MgB_2 tunnel junctions with In counterelectrodes. The peak position between 3 and 4 mV for both polarities indicates the sum of the energy gaps of the MgB_2 film and the In counterelectrode ($\Delta_{In} = 0.5$ meV). Apparently, only a small MgB_2-derived gap $\Delta_s \cong 3$ meV is visible. The tiny shoulder in traces 1, 2, and 3 near ± 7 mV indicates a small contribution of a tunnel current where quasiparticles are sampling the large energy gap. According to calculations of Dolgov *et al.* [16], for tunneling in the c direction of MgB_2, one should observe the tunneling density of states of the π surface, i.e., the small gap, with a small (about 1%) contribution of the large gap from the σ surface. In our experimental data (traces 1, 2, and 3) we estimate the small shoulder to contribute $(2 \pm 1)\%$ to the whole tunnel current. A few junctions (2 out of 50) of this study showed a clear expression of the large gap as shown by the lowest curve (open circles) in Fig. 1. These data indicate a superposition of about equal weight of two tunnel currents sampling the π surface and the σ surface. This situation is expected for tunneling into the ab plane [16]. So far it was experimentally observed for STM tunneling only [9] but not on planar junctions.

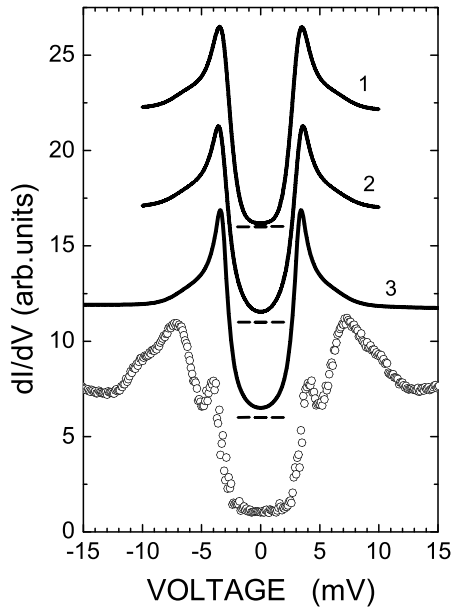

FIG. 1. Differential conductance of 3 junctions (No. 1 to 3) of the type MgB_2/insulator/In showing the small energy gap of MgB_2 (solid lines). Differential conductance of a MgB_2/insulator/Pb junction showing a superposition of the small and the large energy gap of MgB_2 (open circles). All traces were taken at 1.5 K with the counterelectrodes in the superconducting state ($\Delta_{In} = 0.5$ meV, Pb = 1.3 meV). Curves are displaced vertically against each other for clarity. Horizontal bars indicate zero conductance.

In Fig. 2(a) we show the raw tunneling data, i.e., dI/dV versus V, in the superconducting and normal state taken up to voltages where phonon-induced effects are expected. The In counterelectrode was driven normal by a magnetic field of 0.1 T. On the overall increasing background, the trace in the superconducting state shows a stronger increase followed by a leveling-off at three voltages indicated by arrows. These features correspond to relative changes in conductance of a few 10^{-3} and are identified as phonon-induced structures. The steep increase towards low V (below 20 mV) is due to approaching the peaks at the gap edge (see Fig. 1) from the high-voltage end. The increase of the background towards high voltage is caused by inelastic tunneling and by the V dependence of the tunneling matrix element, a situation very similar to junctions on ZrN [13]. The inelastic effects extend up to the very high voltage of 200 mV suggesting that a mixed oxide of Mg and B makes up the tunnel barrier. The small changes of the inelastic background between the normal and superconducting state were included in the evaluation of the tunnel data following the procedure described previously [13].

To demonstrate the phonon-induced effects more clearly and the reproducibility of our data as well, we show in Fig. 2(b) second derivative traces (d^2I/dV^2) for six different junctions taken in the superconducting state after substraction of the normal-state background. The peaks at 39, 58, and 87 mV reflect the features of the dI/dV data and correspond to peaks in the Eliashberg function. Roughly, the peak positions agree with maxima found by Yanson *et al.* [18] in point-contact spectra of MgB_2. It is important to point out that features induced by coupling of electrons to other excitations (here: phonons) appear in the superconductive tunneling conductance if and only if they are responsible for the Cooper pairing mechanism. This is directly demonstrated in the inset of Fig. 2 where the temperature dependence of the tunnel data monitored by the d^2I/dV^2 signal of the largest peak (at 58 mV) is shown. Its vanishing at 32 K, the transition temperature of the film, together with the observation of two gaps in the tunnel data (Fig. 1) confirm both phonon-induced Cooper pairing, in agreement with isotope-effect data [19], and two-band superconductivity in MgB_2. Since the strength of the phonon-induced effect scales in good approximation with the square of the energy gap we also show the square root of the d^2I/dV^2 signal which falls slightly below the BCS temperature dependence for the small gap.

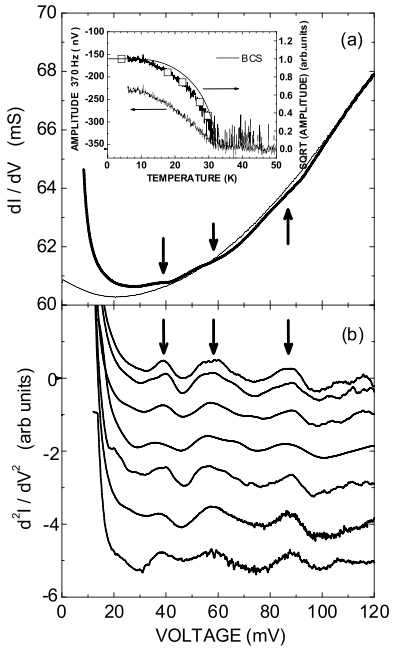

FIG. 2. (a) The raw data of the tunneling experiment dI/dV vs voltage for MgB_2/insulator/In junction No. 1 with the MgB_2 film in the superconducting (bold line) and normal (thin line) state. The arrows indicate the location of phonon-induced features. (b) Second-derivative data taken in the superconducting state of MgB_2 after subtraction of the normal-state background for 6 different junctions. The upper two traces are taken on the same junction (No. 1) with positive and negative voltage bias. The In counterelectrode is driven normal by a magnetic field of 0.1 T. Inset in (a): temperature dependence of the 58 mV structure. The amplitude A of the second derivative signal is shown as measured in a temperature sweep, together with SQRT (A). The strength of the same structure as observed as the steplike feature in the reduced density of states at five different temperatures is also shown (squares). The thin solid line indicates the BCS behavior.

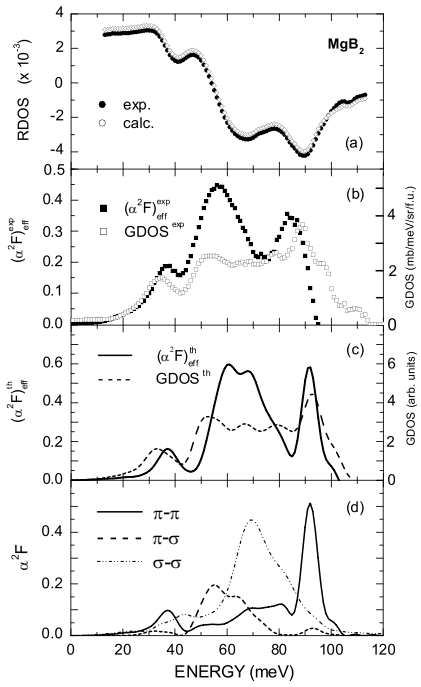

FIG. 3. Analysis of the tunnel data: (a) the reduced density of states (RDOS) of a MgB_2/insulator/In junction (closed symbols) and the fit obtained by standard McMillan-Rowell inversion. (b) Effective Eliashberg function $(\alpha^2F)^{\rm exp}_{\rm eff}$ obtained from the inversion and the generalized experimental phonon density of states (GDOS) [21]. (c) The effective Eliashberg function $(\alpha^2F)^{\rm th}_{\rm eff}$ resulting from McMillan-Rowell inversion of a calculated tunneling density of states of the π surface, and the calculated GDOS. (d) The individual Eliashberg functions for virtual π-π, π-σ, and σ-σ transitions as a result of an *ab-inito* LDA calculation. Included in the calculation is the broadening due to finite phonon lifetimes.

The strategy for the analysis of our tunnel data is the following: with the experimental tunnel data an effective Eliashberg function $(\alpha^2F)^{\rm exp}_{\rm eff}$ was determined using the McMillan-Rowell inversion with single-band Eliashberg equations. A theoretical counterpart$(\alpha^2F)^{\rm th}_{\rm eff}$ was generated using the same inversion code applied to a tunneling density of states of the π band (standing for the small gap) which is calculated by solution of two-band Eliashberg equations [20]. The necessary π-π, σ-σ, and π-σ Eliashberg functions are supplied by an *ab-initio* LDA calculation [6]. Finally, the $(\alpha^2F)^{\rm ex}_{\rm eff}$ and $(\alpha^2F)^{\rm th}_{\rm eff}$ data are compared to extract information on the individual Eliashberg functions $(\alpha^2F)_{\pi\text{-}\pi}$, $(\alpha^2F)_{\sigma\text{-}\sigma}$, and $(\alpha^2F)_{\pi\text{-}\sigma}$. The result of this procedure is depicted in Fig. 3 on a common energy axis (the voltage shifted by the small energy gap). Figure 3(a) shows reduced density of states data resulting from the raw data of Fig. 2 and the very close fit obtained by the inversion calculation. This fit yields the $(\alpha^2F)^{\rm exp}_{\rm eff}$ [Fig. 3(b)]. We observe that it is composed of the three peaks as expected from the d^2I/dV^2 data. For the Coulomb pseudopotential μ^* and the electron-phonon coupling constant, the values 0.1 and 0.65 were obtained.

In Fig. 3(b) we compare our inversion result with the generalized phonon density of states (GDOS) from inelastic neutron-scattering data by Osborn *et al.* [21]. The low energy peaks near 35 meV reflecting mainly magnesium-derived acoustical phonons, and the high-energy peaks near 85 and 89 meV, correspond very well to each other, except for a small shift of about 4 meV between the high-energy peaks, not uncommon for comparisons between tunneling and neutron-scattering data even for simple metals [22]. A possible explanation is strain in the film used for the tunneling experiment. The intensity in the GDOS at high energies above 100 meV is caused by multiphonon contributions. Surprisingly, the largest feature in the tunneling spectrum, the central peak at 58 meV, is not found in the GDOS data which exhibit three shallow maxima between 50 and 80 meV. Such a strong deviation between both quantities and its restriction to a comparably narrow energy range is very unusual. In the past, tunneling and phonon data generally showed a close correspondence over the whole energy range [23].

In Fig. 3(c) we show the theoretical counterparts, i.e., $(\alpha^2F)^{\text{th}}_{\text{eff}}$ (calculated as described above) and the GDOS obtained by the *ab-initio* LDA calculation [6]. We note a striking agreement even for small details between the calculated and experimental phonon data, which lends strong confidence to the LDA calculation. Most importantly, excellent agreement of the characteristic features of the experimental and calculated effective Eliashberg functions with the large central peak as a dominant feature is observed. In order to investigate its origin we show in Fig. 3(d) the three individual Eliashberg functions which emerge from the LDA calculation and which are the input data for the calculation of $(\alpha^2F)^{\text{th}}_{\text{eff}}$. The σ-σ function is fully dominated by only one phonon mode at 72 meV, E_{2g}, which was early discovered theoretically [5,6] as the main driving force for the large gap on the σ surface. Turning to the π-π and π-σ functions, we observe a peculiar "energy selectivity." The π-σ function shows most intensity between 50 and 70 meV where the π-π function is weakest. The phonon modes in this energy region are characterized by out-of-plane motions of the boron atoms. Obviously the virtual transitions of quasiparticles between the two-dimensional σ bands and the three-dimensional π bands are almost exclusively coupling to these phonons whereas magnesiumlike phonons and higher-energy optical modes including the E_{2g} are not effective for interband transitions. An analysis of the two-band Eliashberg equations shows that the gap function of the π sheet rendering $(\alpha^2F)^{\text{th}}_{\text{eff}}$ is essentially determined by the π-π and π-σ functions. It shows further that the interband π-σ function is shifted to larger energy by the difference of the energy gaps and, most importantly, is increased by a weighting factor given by the ratio of the gaps. Both of these features reflect the peculiarities of interband electron-phonon interaction, where within the self-energy interpretation of the Eliashberg equations, a quasiparticle virtually passes from the π surface over to the σ surface and decays to the edge of the large gap. Indeed, $(\alpha^2F)^{\text{th}}_{\text{eff}}$ of Fig. 3(c) can be reproduced to a good approximation by a superposition of the π-π and the π-σ function if the latter is shifted to higher energy by 5 meV (the difference of the energy gaps in the calculation) and is multiplied by a factor of about three, the ratio of the energy gaps. This generates the large central peak in $(\alpha^2F)^{\text{th}}_{\text{eff}}$. Hence the large central peak in the experimental data reflects the shape of the interband π-σ Eliashberg function. Its effect on the superconductivity of the π surface is dramatic. The π-π function yields for the electron-phonon coupling constant λ the value of 0.25, not enough to account for superconductivity on the π sheet of MgB_2. The increase of λ to a value of 0.65 and hence the very existence of the small energy gap on the π surface is caused by the π-σ function and its augmented weight.

In conclusion, the strong-coupling effects in the tunneling density of states of a two-band superconductor, MgB_2, have been determined and analyzed. Effective Eliashberg functions were generated by combining two-band Eliashberg theory and *ab-initio* LDA calculations and compared to the experimental data. The main result is that it is the interband pairing interaction that gives rise to the dominating feature, a strong peak at 58 meV, in the effective Eliashberg function of the π sheet. It is due to a selectivity of the π-π transitions and π-σ transitions of the quasiparticles for the modes of the involved phonons. For the interband transitions almost exclusively, phonons on the low-energy end of the optical spectrum, characterized by out-of-plane movements of boron atoms, are effective.

[1] H. Suhl, B. T. Matthias, and L. R. Walker, Phys. Rev. Lett. **3**, 552 (1959).
[2] G. Binnig, A. Baratoff, H. E. Hoenig, and J. G. Bednorz, Phys. Rev. Lett. **45**, 1352 (1980).
[3] J. Nagamatsu, N. Nakagawa, T. Muranaka, Y. Zenitani, and J. Akimitsu, Nature (London) **410**, 63 (2001).
[4] F. Bouquet *et al.*, Phys. Rev. Lett. **89**, 257001 (2002); D. G. Hinks, H. Claus, and J. D. Jorgensen, Nature (London) **411**, 457 (2001).
[5] J. M. An and W. E. Pickett, Phys. Rev. Lett. **86**, 4366 (2001).
[6] K.-P. Bohnen, R. Heid, and B. Renker, Phys. Rev. Lett. **86**, 5771 (2001).
[7] H. J. Choi, D. Roundy, H. Sun, M. L. Cohen, and S. G. Louie, Nature (London) **418**, 758 (2002).
[8] A. Y. Liu, I. I. Mazin, and J. Kortus, Phys. Rev. Lett. **87**, 87005 (2001).
[9] M. Iavarone *et al.*, Phys. Rev. Lett. **89**, 187002 (2002).
[10] F. Laube, G. Goll, J. Hagel, H.v. Löhneysen, D. Ernst, and T. Wolf, Europhys. Lett. **56**, 296 (2001).
[11] S. Tsuda *et al.*, Phys. Rev. Lett. **91**, 127001 (2003).
[12] W. L. McMillan and J. M. Rowell, Phys. Rev. Lett. **14**, 108 (1965).
[13] J. Geerk, U. Kaufmann, W. Bangert, and H. Rietschel, Phys. Rev. B **33**, 1621 (1986); J. Geerk, G. Linker, and R. Smithey, Phys. Rev. Lett. **57**, 3284 (1986) and references therein.
[14] R. Schneider, J. Geerk, and H. Rietschel, Europhys. Lett. **4**, 845 (1987).
[15] A. Brinkman, A. A. Golubov, H. Rogalla, O. V. Dolgov, J. Kortus, Y. Kong, O. Jepsen, and O. K. Andersen, Phys. Rev. B **65**, 180517(R) (2002).
[16] O. V. Dolgov *et al.*, Phys. Rev. B **68**, 132503 (2003).
[17] R. Schneider, J. Geerk, F. Ratzel, G. Linker, and A. G. Zaitsev, Appl. Phys. Lett. **85**, 5290 (2004).
[18] I. K. Yanson *et al.*, Phys. Rev. B **67**, 024517 (2003).
[19] D. G. Hinks, H. Claus, and J. D. Jorgensen, Nature (London) **411**, 457 (2001).
[20] F. Marsiglio, M. Schossmann, and J. P. Carbotte, Phys. Rev. B **37**, 4965 (1988).
[21] R. Osborn, E. A. Goremychkin, A. I. Kolesnikov, and D. G. Hinks, Phys. Rev. Lett. **87**, 017005 (2001).
[22] J. M. Rowell, W. L. McMillan, and W. L. Feldmann, Phys. Rev. **178**, 897 (1969).
[23] E. L. Wolf, *Principles of Electron Tunneling Spectroscopy* (Oxford University Press, New York, 1985).